Coverage Effect of Self-Assembled Polar Molecules on the Surface Energetics of Silicon

ARTICLE *in* THE JOURNAL OF PHYSICAL CHEMISTRY C · JULY 2008

Impact Factor: 4.77 · DOI: 10.1021/jp805723u

Tailoring the Work Function of Gold Surface by Controlling Coverage and Disorder of Polar Molecular Monolayers

Nira Gozlan, Ulrike Tisch, and Hossam Haick*

The Department of Chemical Engineering and Russell Berrie Nanotechnology Institute, Technion-Israel Institute of Technology, Haifa 32000, Israel

Received: April 10, 2008; Revised Manuscript Received: June 4, 2008

We show here that the work function of Au can be controlled not only by the magnitude and direction of adsorbed polar molecules but also by the molecular coverage and (dis)order within the molecular patterns. Molecular monolayers composed of two types of molecules with opposite dipoles were deposited on Au films containing the changes of the work function due to variation of molecular coverage and disorder were monitored. The results indicate that the requirements on molecular layers covering Au surfaces are significantly relaxed and that partial, disordered monolayers can be used to tailor the work function of metal surfaces.

1. Introduction

The design, preparation, and study of the physical properties of molecular assemblies and organic molecule-based materials with specific properties are an active area of research.[1–4] The quest in this area is not only for molecule-based compounds that behave as classical materials but also to produce materials and systems with novel properties. By wise choice of the molecular building blocks one can in principle combine, in the same crystalline framework, specific properties that are difficult to achieve in a one-phase solid.[1,5]

Adsorption of tailormade organic molecules onto solid electronic surfaces can lead to hybrid molecular/nonmolecular systems that combine the cooperative (electron transport) properties of the solids with the controllable functional versatility of the molecules.[5–9] While advances in this field depend on the electrical controllability of solid surfaces, doing so in a facile and reproducible fashion is often a combination of science, technology, and art. The relative importance of the science and art depends on how far the technology and our understanding have advanced. It is, therefore, not surprising that adsorbing molecules on solid electronic surfaces to introduce new electrical characteristics severely affects the realization of hybrid devices. This is due mostly to limited understanding of the interaction(s) between the solid surfaces and the different parts of the molecules,[5,6,10,11] especially at different molecular coverage. Such understanding is critical for knowing how details of adsorption, in terms of materials and methods, affect the resulting molecule-based device characteristics.

Recent studies have shown that chemisorption of a polar self-assembled monolayer (SAM) on the surface of a metal electrode can be used to lower the energy barrier for charge injection and thus increase device performance.[12–15] The importance of this type of chemisorption is also clear from research on organic thin film devices, e.g., field effect transistors[16,17] and photovoltaic cells,[18] where understanding the effect of the polar molecules is crucial. For example, Campbell et al. demonstrated that polar arenethiol SAMs with opposite dipole moments could be used to change the work function of copper in opposite directions in a predictable manner.[14] Providing the low effective tunneling barrier for electron transfer in SAMs derived from *n*-alkanethiols, the authors explained their observations by the presence of dense and well-ordered monolayers.[19,20] On the other hand, defect sites, which can contribute to changes in work function in an unpredictable manner, were found to be "patched" through a process involving subsequent adsorption of hexadecanethiol (HDT).[20] An acceptable explanation for these effects is based on considering the molecular layer as a dipole layer with long-range interactions[21] and, in some cases, actual charge transfer with the substrate.[5,22]

Electrical interactions between metals and organic molecules and polymers have been studied extensively by in situ ultraviolet photoemission spectroscopy (UPS), X-ray photoelectron spectroscopy (XPS), and Kelvin probe measurements following deposition of molecules on metallic substrates and metal layers on organic thin films.[12,23,24] These techniques show that molecules interact with the metal via metal polarization, coupling of electronic states, partial charge exchange (i.e., ionic bond formation), or formation of new chemical species,[12,23,24] affecting the alignment of the energy levels at the interface and as the charge transport through it.

Here we investigate the structural requirements of the molecular subunit and polar SAM for tuning the work function. We studied the changes in the work function of Au films containing function of molar coverage (ranging from ~10% to 98%) with negative and positive polar SAMs. The electrical characteristics were correlated with the microscopic (dis)order, density of defect sites, and adsorption patterns within the monolayer obtained by scanning tunneling microscopy (STM) images.

2. Experimental Section

2.1. Materials. Gold (Au), titanium (Ti), and copper (Cu) metals with >99% purity were purchased from Kurt J. Lesker, USA. Four inch double-side polished n-type (100) silicon (10^{15} cm^{-3}) wafers with roughness < 1 nm were purchased from Silicon Quest International, Inc. (Santa Clara, CA).

2.2. Sample Preparation. Si substrates were cleaned by sequential immersion for 1 min each in a sonicated bath of methanol, acetone, methylene chloride, 1,1,1-trichloroethane, methylene chloride, acetone, and methanol. The sample was then subjected to a final rinse with 18 MΩ deionized water, dried under a stream of nitrogen, and treated with ozone

* E-mail: hhossam@technion.ac.il.

10.1021/jp803124j CCC: $40.75
Published on Web 07/25/2008

oxidation for 20 min in a UVOCs apparatus. The native oxide was etched from the clean wafers for 30 s in buffered $HF_{(aq)}$ (pH = 5−6, 5:1 (v/v) $NH_4F/HF_{(aq)}$).[25] After removal from the etching solution, the sample was rinsed thoroughly with 18 MΩ deionized water for 30 s and dried under a stream of nitrogen.

Following the cleaning procedure, the wafers were transferred to an inert glovebox working with dry nitrogen with a closed cycle purification system (<1 ppm O_2 and <1 ppm H_2O) and integrated with an e-beam evaporator TFDS-870 (Vacuum Systems & Technologies Ltd., Israel), where further processes were carried out. The TFDS-870 allows deposition of controllable multilayers with a choice of six different materials without braking vacuum. A 200 nm Au film containing 2.4% Cu (hereinafter, Cu(2.4%)/Au) was produced by e-beam coevaporation on the ultraflat Si substrates[26] at $1-6 \times 10^{-5}$ Torr. Cu(2.4%)/Au films were deposited on 10−20 nm Ti layer to increase the adhesion of the metallic layer to the Si substrate. The deposition rate was kept below 1−2 Å/s in order to obtain a film surface with minimum roughness and to minimize undesired substrate heating. After metal deposition, the organic monolayers were adsorbed on the surface of the Cu(2.4%)/Au-coated substrates inside the glovebox without exposing the samples to air. The introduction of minute amounts of Cu in the Au film results in a coalescence of the fine-scale Au grains into larger ones, hence improving the packing density and stability of the adsorbed SAMs.[27,28]

Monolayers of hexadecanethiol ($HS-(CH_2)_{15}-CH_3$; HDT) and 16-mercaptohexadecanoic acid ($HS-(CH_2)_{15}-CO_2H$; MHD) with varied surface coverage (∼10−98%) were formed by immersing the bare Cu(2.4%)/Au samples in a 1 mM solution of the alkanethiols in ethanol for different immersion times, ranging between 2 min and 24 h. Then the samples were removed from the adsorption solutions, rinsed and sonicated for 1 min in pure ethanol in order to remove all loosely bound molecules, and dried in a flow of nitrogen. Thereafter, the SAM-covered Cu(2.4%)/Au surfaces were exposed to ambient air conditions during and between the various characterization steps.[29]

2.3. Kelvin Probe Measurements. Contact potential difference (CPD) was determined under ambient conditions (293 K, 40% relative humidity) with the Ambient Kelvin Probe Package of KP Technology Ltd. by measuring the electrical potential of contact-free surfaces relative to that of a (Au) reference. The KP package includes a head unit with integral tip amplifier, a 2 mm tip, a PCI data acquisition system, a digital electronics module, the system software, an optical baseboard with sample and Kelvin probe mounts, a 1 in. manual translator, and a Faraday cage. The work function resolution of the system is 1−3 mV. Data was collected for three or more different samples and averaged.

2.4. Quantum Chemical Calculations. Density functional theory (DFT) calculations using the GO3W package with the B3LYP method and 6-311G basis set were used to calculate the dipole moment and length of free HDT and MHD molecules.

2.5. Scanning Tunneling Microscopy (STM). STM measurements were performed using a UHV/VT AFM Omicron system and a commercially available tungsten tip, which was cleaned in UHV to remove the tungsten oxide prior to use. All STM images were obtained at a constant bias voltage of 1 V and a tunneling current of 0.15 nA between the tip and the sample. No structural defects or transitions were observed during the STM imaging, indicating that the SAM structures were not affected by the STM tip.

2.6. Fourier Transform Infrared Spectroscopy (FTIR). Fourier transform infrared (FTIR) spectra between 400 and 4000 cm^{-1} were recorded with a Bruker IFS55 (Bruker Optik GmbH, Germany) inside a sample compartment having controlled temperature and environment. SAMs on IR-opaque substrates (i.e., Cu(2.4%)/Au) were measured with a specular reflectance accessory at grazing angle.

2.7. Spectroscopic Ellipsometery. Ellipsometric spectra were recorded over a range from 250−1000 nm at three different incidence angles 65°, 70°, and 75° using a spectroscopic phase modulated ellipsometer (M-2000V Automated Angle, J. A. Woollam Co., Inc.). The optical constants of the Cu(2.4%)/Au Si substrates were determined experimentally from a reference sample. We use a two-phase SAM/substrate model to extract the thickness of the SAM layer. An absorption-free Cauchy dispersion of the refractive index with values of n between 1.46 at 1000 nm and 1.61 at 250 nm was assumed for all SAM layers.

3. Results and Discussion

To assess the effects of the actual coverage of the organic dipoles we prepared and characterized a series of molecularly modified Cu(2.4%)/Au surfaces with monolayer coverage, N, ranging from 10% to 98%. Figure 1 shows representative STM images of HDT monolayers that were deposited by immersing the Cu(2.4%)/Au substrate in HDT solution for varying amounts of time.[30] Initially, at ∼36% coverage (Figure 1b) the HDT were arranged in disordered islands. These islands then served as centers for aggregation of molecules diffusing on the surface as well as for adsorption from solution.[30] The size and height of the islands increased with increasing surface coverage, indicating that HDT molecules changed their tilting continuously. That is so because molecules lying flat on the surface gradually grew two dimensionally to the standing-up phase as the surface coverage is increased after dipping for longer times. Domain-like structures (i.e., pinholes) were observed at ∼73% coverage. At higher coverage (Figure 2c), the pinholes between the islands shrank and eventually a continuous and ordered SAM was formed (Figure 1d−e).[31] At ∼98% coverage (Figure 1e) most of the surface was covered with closely packed molecules. Most boundaries had three directions originating from the Cu(2.4%)/Au(111) surface symmetry. The boundaries were terminated by either the Cu(2.4%)/Au(111) step edges or other boundaries. The origin of the monoatomic depth (∼2.4 Å) is not well understood yet but is probably related to clustering of the Au defects during dipping in the solution and stabilization of these structures by closely packed SAMs.[32,33]

Analysis of the ellipsometric spectra of the various samples confirmed the STM observations. As could be observed in Table 1 the thickness extracted from the ellipsometric spectra increased with increasing the surface coverage. This can easily be understood if one considers that ellipsometry probes a macroscopic section of the surface (in our instrument 1−3 mm^2, depending on the angle of incidence). Therefore, the extracted effective thickness, $d_{eff} \approx NL\cos(\theta)$, is a macroscopic average over a large surface area, which is in part covered with molecules of length, L, inclined at an angle, θ, with respect to the surface normal. The effective thickness of HDT molecules having almost full coverage ($d_{eff} = 2.4 \pm 0.5$ nm) agreed reasonably well with the DFT calculation of the molecular length ($L = 2.1$ nm) within the margin of error. However, the effective thickness of MHD molecules having almost full coverage ($d_{eff} = 2.7 \pm 0.1$ nm) slightly exceeded the molecular length calculated using DFT ($L = 2.2$ nm). This discrepancy may be due to a slight underestimation of the refractive index. Note,

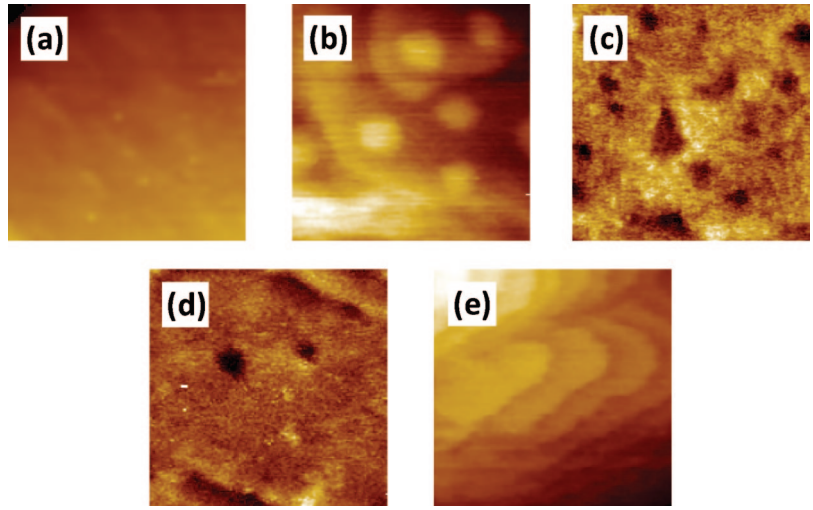

Figure 1. STM images showing several phases formed in the self-assembly processes of HDT on Cu(2.4%)/Au at different coverage: (a) 0% (bare sample), (b) ~36%, (c) ~73%, (d) ~92%, and (e) ~98%. The thickness of the "white" spots in image a is ~0.1 nm, indicating minute contaminations on the surface of bare sample. The thickness of "islands" in image b is comparable to the thickness obtained by ellipsometery (1.1 ± 0.1 nm) and, therefore, can be attributed to HDT "islands". The scale in all images is 30 nm × 30 nm.

TABLE 1: Thickness of MHD and HDT Monolayers at Varied Surface Coverage As Determined by Spectroscopic Ellipsometery

MHD		HDT	
coverage [%]	thickness [nm]	coverage [%]	thickness [nm]
34 ± 4	1.0 ± 0.4	56 ± 4	1.3 ± 0.3
39 ± 5	1.1 ± 0.1	60 ± 2	1.3 ± 0.5
56 ± 4	1.6 ± 0.2	66 ± 3	1.6 ± 0.1
67 ± 2	1.9 ± 0.1	72 ± 3	1.7 ± 0.1
77 ± 3	2.1 ± 0.1	76 ± 3	1.8 ± 0.1
83 ± 4	2.3 ± 0.3	86 ± 4	2.1 ± 0.1
86 ± 3	2.4 ± 0.2	98 ± 2	2.4 ± 0.5
98 ± 2	2.7 ± 0.1		

that an exact determination of the absolute thickness of nanometer thick layers by spectroscopic ellipsometry is somewhat challenging. Also, assuming isotropic optical constants for a layer composed of separate polar molecules may introduce experimental error. Furthermore, the approximations in quantum mechanical DFT calculations may introduce an error into the calculated values, which is difficult to estimate.

For thiolated SAMs on Cu(2.4%)/Au the C−H stretching region of the FTIR spectra was used as a diagnostic for methylene chain ordering at different surface coverage. Typically, in spectroscopic techniques like FTIR the average over macroscopic lengths is often particularly sensitive to the tilt angle of the molecular backbone. These techniques detect molecules in disordered and ordered areas no matter whether they are strongly attached to the substrate or not. This can lead to an effective decrease of the determined overall tilt angle. With these differences in mind it seems that the partially formed films consisted of islands with essentially upright molecules and in between (possibly not yet strongly bound) molecules with larger tilt angles.[30] Previous studies have shown that crystalline polyethylene, which is characterized by a low concentration of gauche defects, the symmetric (d^+) and antisymmetric (d^-) methylene stretching vibrations lie at 2850 and 2918 cm^{-1}, respectively.[34,35] Several reports have shown similar values for ordered alkylthiol chains with chains longer than C_6,[36] higher values for liquid-like alkanes with chains shorter than C_6,[34,35] and smaller ones for highly crystalline SAMs with chains longer than C_{20}.[34,35] For HDT and MHD on Cu(2.4%)/Au films, the gauche defect population showed a nonmonotonic change with the molecular coverage and reaches a saturation level at a critical coverage. More specifically, the d^- stretch decreased from 2922 cm^{-1} at 10−20% coverage to 2918 cm^{-1} at a critical coverage (~86%), indicating a transformation from the disordered, liquid-like phase to an ordered one.[34–36] The same stretching mode was stabilized at 2918 cm^{-1}, indicating the ordered phase at values higher than the critical coverage of the studied SAMs. Comparing the STM and FTIR results in this region of surface coverage showed that varied concentrations of small pinholes (1−3 nm in diameter) have no sizable effect on the order within the SAM films.

The change of the work function, Φ, with respect to that of the Au/Cu reference was determined for samples similar to those used in the STM and FTIR analysis. For molecules on a metal surface ΔΦ can be expressed as follows[37]

$$\Delta\Phi = \frac{N\mu \cos\theta}{\varepsilon\varepsilon_o} \quad (1)$$

Here μ is the molecule's dipole moment, N is the density of adsorbed molecules, θ is the average tilt of molecules relative to the surface normal, ϵ is the effective dielectric constant of the molecular film (including any depolarization effects[6]), and ϵ_o is the permittivity of free space. The SAMs, HDT and MHD molecules used in this study have a common C_{15} alkyl backbone and thiol groups for binding to the Cu(2.4%)/Au surface but differ in the functional groups (CH_3 vs COOH) pointing outward, thus modifying the electron-donating/withdrawing power. Density functional theory (DFT) calculations yielded a dipole moment of $\mu = -2.1 \pm 0.3$ D and $+2.5 \pm 0.3$ D for HDT and MHD molecules, respectively. In work function measurements, the quantity $(\mu \cos\theta)/\varepsilon$ is often referred to as the effective dipole moment, μ_{eff}, since experimentally determined dielectric constants of monolayers are often several times greater than those observed in bulk materials of similar composition. This disparity may be the result of dipole interaction between neighboring molecules or disorder in the film that allows the dipoles to tilt away from the surface normal.

The work function varied with the free molecules' dipole moments, in agreement to previous reports.[38] The covered metal surfaces showed clear but opposite effects of the molecule substituent on the Φ characteristics (Figure 2). Negative molecular dipoles (HDT; −2.1 ± 0.3 D) decreased Φ of

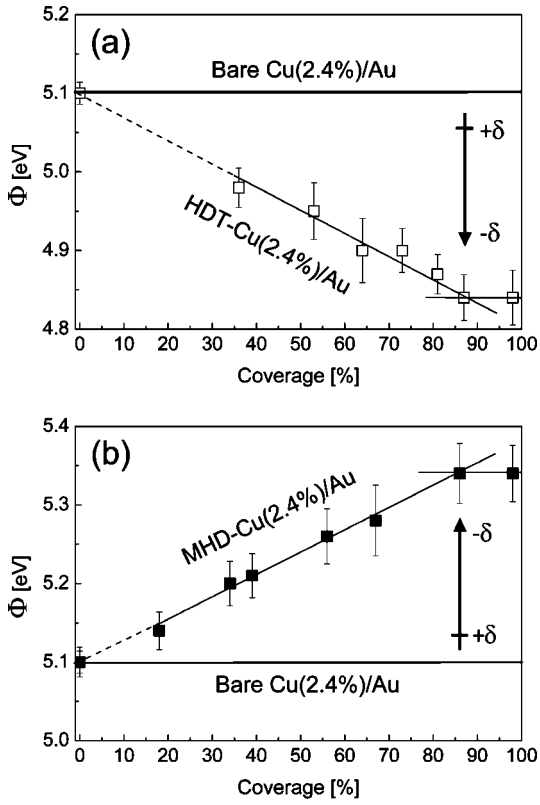

Figure 2. Work function (Φ) of Cu(2.4%)/Au substrates as a function of (a) HDT and (b) MHD coverage. At zero coverage (i.e., bare Cu(2.4%)/Au), the work function stands on 5.1 ± 0.1 eV. The presented data is averaged from at least three different samples.

SCHEME 1: Schematics of (a) Hexadecanethiol ($HS-(CH_2)_{15}-CH_3$; HDT) and (b) 16-Mercaptohexadecanoic Acid ($HS-(CH_2)_{15}-CO_2H$; MHD) Molecules on Au as well as the Related Dipole Moment Vectors, which Are Oriented from the + to the − Charge[46–50] [a]

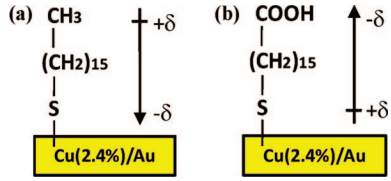

[a] The dipole is defined as positive if its positive pole is closest to the substrate. The calculated dipole moment of the HDT and MHD molecules is −2.1 ± 0.3 D and +2.5 ± 0.3 D, respectively. The calculated length of the HDT and MHD molecules is 2.1 and 2.2 nm, respectively.

Cu(2.4%)/Au at a given coverage (Figure 2a), and positive molecular dipoles (MHD; +2.5 ± 0.3 D) increased it (Figure 2b). **NOTE:** The dipole is defined as positive if its positive pole is closest to the substrate (see Scheme 1). For SAMs on Au(111) it has been shown that the dipole moment density is mainly determined by the permanent dipoles in the thiolate molecular layer. The polarity of the sulfur−gold bonds that are formed upon adsorption (<0.1 D) is almost negligible when compared to the polarity of the molecules and, therefore, gives only a small contribution to the interface dipole.[39] The charge transfer in these materials is small and plays a negligible role in the interfacial electrostatics.[39,40]

At zero coverage, the work function of the Cu(2.4%)/Au substrate was determined to be 5.1 ± 0.1 eV, in good agreement with previously reported values of Au.[7,9,41] This good agreement indicated that neither the inclusion of 2.4% Cu nor the underlying Si substrate had a measurable effect on the work function of the bare Cu(2.4%)/Au sample.[42] From Figure 2a one can also observe that upon deposition of HDT the Φ decreases monotonically by 0.26 eV, reaching 4.84 eV at 86% critical coverage. Upon deposition of MHD, Φ increased monotonically by 0.24 eV, reaching 5.34 eV at a critical coverage of 86% (see Figure 2b). ΔΦ is likely due to a partial electron transfer from the MHD molecules, which are electron donors, to the Cu(2.4%)/Au surface atoms upon chemisorptions and vice versa for the HDT molecules. The charge redistribution created a chemical dipole that contributes, together with the modification of the electronic density at the metal surface, to the overall interface dipole when a monolayer is chemisorbed on Au. From the critical coverage on, until reaching almost full coverage, the work functions of the SAMs on Cu(2.4%)/Au did not depend strongly upon the coverage of the molecules. Structures with packing density that differed by ∼14% had a similar work function, within the margin of error (4.84 eV for HDT and 5.34 eV for MHD). This is slightly surprising since one expects the shift in the work function upon adsorption of the SAM to depend on the packing density of the molecules. On one hand, one would expect a higher coverage to result in a larger work function shift because of a higher density of molecular dipoles (eq 1). On the other hand, increasing the coverage of the molecular dipoles also enlarges the depolarizing field in the SAM, which acts to decrease the dipoles and, therefore, the work function shift. Apparently in the range of packing densities that are relevant to ∼86% MHD and HDT coverage structures these two effects tend to cancel one another.[39] This effect is verified empirically using an effective dielectric constant for the molecular layer. To confirm this idea we used the correlation shown in eq 1 and extracted the experimental values of μ, viz. the "effective dipole moment" (μ_{eff}). The results show that up to the critical coverage (86% MHD and HDT) μ_{eff} is (roughly) constant and equal to +2.8 ± 0.6 D for MHD and −2.9 ± 0.5 D for HDT. The dipole moment calculated using DFT for MHD, μ = +2.5 ± 0.3 D, lies within the margin of error of the experimental value. The one calculated for HDT, μ = −2.1 ± 0.3 D, is somewhat lower, which may be due an inaccuracy in the calculation. Note that approximations are used in quantum mechanical DFT calculations, which may affect the accuracy of the results.

Obviously, a molecular polar layer is different from a textbook parallel plate capacitor.[43] On the scale of interatomic distances, even a perfectly ordered layer of polar molecules is a quantum mechanical object with rapid variations in charge density along both the lateral and the vertical directions. Up close, the electric field distribution of a molecular layer is quite different from that of a classical parallel plate capacitor with its charge assumed to be perfectly smeared out in the lateral directions. These marked differences immediately raise two questions: First, do the above-described experimental observations suggest that a more realistic view of ideal monolayers needs to be adopted? Second, to what extent can we still rationalize the experimental results semiclassically, albeit with a refined model, and where, if at all, are we observing inherently quantum effects? To answer these questions, we offer here a qualitative analysis of the electrostatics of polar monolayers.[6]

When an array of dipoles is assembled, the potential and electric field simply adds up according to the superposition principle. However, it is important to remember that molecules are polarizable, and therefore, their net dipole moment may change in response to external electric fields, such as those due

to dipoles of other molecules. Recent findings[7,39,44,45] revealed that a depolarization, i.e., a reduction of the molecular dipole with respect to its gas-phase value, is expected. Each molecule experiences an electric field due to the dipoles of all other molecules, which points in a direction opposite to that of the molecule's own dipole. The remaining major question is what electrical potential is generated by an *array* of (possibly partially depolarized) dipoles. Recent calculation have shown that for an infinite, periodic 2D array of dipoles, either a point dipole or a finite dipole, outside the dipolar sheet the potential rapidly converges to a constant because of the rapidly decaying exponential terms. Potential changes due to different polar groups, however, might be observed because the dielectric response is not microscopically uniform. Especially for periodic monolayers with low molecular coverage, where significant electric fields can exist, lateral averaging can grossly underrepresent the extent of field and, similarly, the extent of charge transfer between substrate and molecule.

Summary and Conclusions

Our results provide experimental evidence that systematic control of the work function of metals can be achieved by controlling not only the properties of the molecular dipoles but also their coverage on the surface. The only condition to be fulfilled is that, on the average, the adsorbed molecules will have some degree of disorder within the film. Complete order within the SAM film, even at partial coverage and existence of small pinholes, will lead to depolarization[6] and the surface coverage will stop playing a role in controlling the metal's work function. Putting these results in a wider prospective, the requirements on the molecule on Au surfaces (or contacts) are significantly and nearly completely relaxed. The work function can be controlled by partial, disordered monolayers. Therefore, the ability of the molecules to form pinhole-free coverage will not be important. In addition, formation of laterally inhomogeneous molecular layers is in the direction of and may lay the foundation for implementation of multiple functions on hard or flexible substrates with lateral resolution down to tens of nanometers.

Acknowledgment. We acknowledge the Marie Curie Excellence Grant of the FP6, the US-Israel Binational Science Foundation, and the Russell Berrie Nanotechnology Institute for financial support and Dr. Cecile Saguy from UHV/VT SPM laboratory of the Technion for the STM measurements. H.H. holds the Horev Chair for Leaders in Science and Technology.

References and Notes

(1) Seker, F.; Meeker, K.; Kuech, T. F.; Ellis, A. B. *Chem. Rev.* **2000**, *100*, 2505.
(2) Cahen, D.; Hodes, G. *Adv. Mater.* **2002**, *14*, 789.
(3) Heath, J. R.; Ratner, M. A. *Phys. Today* **2003**, *56*, 43.
(4) Haick, H. *J. Phys. D* **2007**, *40*, 7173.
(5) Ashkenasy, G.; Cahen, D.; Cohen, R.; Shanzer, A.; Vilan, A. *Acc. Chem. Res.* **2002**, *35*, 121.
(6) Natan, A.; Kronik, L.; Haick, H.; Tung, R. T. *Adv. Mater.* **2007**, *19*, 4103.
(7) Heimel, G.; Romaner, L.; Zojer, E.; Bredas, J. L. *Nano Lett.* **2007**, *7*, 932.
(8) Rusu, P. C.; Brocks, G. *Phys. Rev. B* **2006**, *74*, 073414.
(9) Alloway, D. M.; Hofmann, M.; Smith, D. L.; Gruhn, N. E.; Graham, A. L.; Colorado, J., R.; Wysocki, V. H.; Lee, R. T.; Lee, P. A.; Armstrong, N. R. *J. Phys. Chem. B* **2003**, *107*, 11690.
(10) Haick, H.; Cahen, D. *Acc. Chem. Res.* **2008**, *41*, 359.
(11) Haick, H.; Cahen, D. *Prog. Surf. Sci.* **2008**, *83*, 217.
(12) Ishii, H.; Sugiyama, K.; Ito, E.; Seki, K. *Adv. Mater.* **1999**, *11*, 605.
(13) Campbell, I. H.; Rubin, S.; Zawodzinski, T. A.; Kress, J. D.; Martin, R. L.; Smith, D. L.; Barashkov, N. N.; Ferrariis, J. P. *Phys. Rev. B* **1996**, *54*, R14321.
(14) Campbell, I. H.; Kress, J. D.; Martin, R. L.; Smith, D. L.; Barashkov, N. N.; Ferraris, J. P. *Appl. Phys. Lett.* **1997**, *71*, 3528.
(15) de Boer, B.; Hadipour, A.; Mandoc, M. M.; Van Woudenbergh, T.; Blom, P. W. M. *Adv. Mater.* **2005**, *17*, 621.
(16) Shen, Y.; Hosseini, A. R.; Wong, M. H.; Malliaras, G. G. *ChemPhysChem* **2004**, *5*, 16.
(17) Hirose, Y.; Kahn, A.; Aristov, V.; Soukiassian, P.; Bullovic, V.; Forrest, S. R. *Phys. Rev. B* **1996**, *54*, 13748.
(18) Gal, D.; Sone, E.; Cohen, R.; Hodes, G.; Libman, J.; Shanzer, A.; Schock, H. W.; Cahen, D. *Proc. Indian Acad. Sci., Chem. Sci.* **1997**, *109*, 487.
(19) Dhirani, A.-A.; Zehner, R. W.; Hsung, R. P.; Guyot-Sionnest, P.; Sita, L. R. *J. Am. Chem. Soc.* **1996**, *118*, 3319.
(20) Zehner, R. W.; Sita, L. R. *Langmuir* **1997**, *13*, 2973.
(21) Vilan, A.; Ghabboun, J.; Cahen, D. *J. Phys. Chem. B* **2003**, *107*, 6360.
(22) Schlettwein, D.; Hesse, K.; Gruhn, N. E.; Lee, P. A.; Nebesny, K. W.; Armstrong, N. R. *J. Phys. Chem. B* **2001**, *105*, 4791.
(23) Kahn, A.; Koch, N.; Gao, W. *J. Polym. Sci. B* **2003**, *41*, 2529.
(24) Shen, C.; Kahn, A.; Schwartz, J. *J. Appl. Phys.* **2001**, *90*, 6236.
(25) Nemanick, E. J.; Hurley, P. T.; Brunschwig, B. S.; Lewis, N. S. *J. Phys. Chem. B* **2006**, *110*, 14800.
(26) Liedberg, B.; Wirde, M.; Tao, Y.-T.; Tengvall, P.; Gelius, U. *Langmuir* **1997**, *13*, 5329.
(27) Twardowski, M.; Nuzzo, R. G. *Langmuir* **2002**, *18*, 5529.
(28) Chen, I.-W. P.; Chen; C.-C; Lin, S.-Y. C., C. -H. *J. Phys. Chem. B* **2004**, *108*, 17497.
(29) Liedberg, B.; Wirde, M.; Tao, Y.-T.; Tengvall, P.; Gelius, U. *Langmuir* **1997**, *13*, 5329.
(30) Schwartz, D. K. *Annu. Rev. Phys. Chem.* **2001**, *52*, 107.
(31) Similar STM images were observed for the MHD on Cu(2.4%)/Au (not shown).
(32) Ohgi, T.; Sheng, H.-Y.; Dong, Z.-C.; Nejoh, H. *Surf. Sci.* **1999**, *442*, 277.
(33) Delamarche, E.; Michel, B.; Kang, H.; Gerber, C. T. *Langmuir* **1994**, *10*, 4103.
(34) Snyder, R. G.; Strauss, H. L.; Elliger, C. A. *J. Phys. Chem.* **1982**, *86*, 5145.
(35) Snyder, R. G.; Maroncelli, M.; Strauss, H. L.; Hallmark, V. M. *J. Phys. Chem.* **1986**, *90*, 5623.
(36) Porter, M. D.; Bright, T. B.; Allara, D. L.; Chidsey, C. E. D. *J. Am. Chem. Soc.* **1987**, *109*, 3559.
(37) Moench, W. *Semiconductor surfaces and interfaces*, 3rd ed.; Springer-Verlag: Berlin, Germany, 2001.
(38) Zehner, R. W.; Parsons, B. F.; Hsung, R. P.; Sita, L. R. *Langmuir* **1999**, *15*, 1121.
(39) Rusu, P. C.; Brocks, G. *J. Phys. Chem. B* **2006**, *110*, 22628.
(40) Konôpka, M.; Rousseau, R.; Stich, I.; Marx, D. *J. Am. Chem. Soc.* **2004**, *126*, 12103.
(41) de Boer, B.; Frank, M. M.; Chabal, Y. J.; Jiang, W.; Garfunkel, E.; Bao, Z. *Langmuir* **2004**, *20*, 1539.
(42) Bruening, M.; Cohen, R.; Guillemoles, J. F.; Moav, T.; Libman, J.; Shanzer, A.; Cahen, D. *J. Am. Chem. Soc.* **1997**, *119*, 5720.
(43) Kronik, L.; Shapira, Y. *Surf. Sci. Rep.* **1999**, *37*, 1.
(44) Gershewitz, O.; Sukenik, C. N.; Ghabboun, J.; Cahen, D. *J. Am. Chem. Soc.* **2003**, *125*, 4730.
(45) Fukagawa, H.; Yamane, H.; Kataoka, T.; Kera, S.; Nakamura, M.; Kudo, K.; Ueno, N. *Phys. Rev. B* **2006**, *73*, 245310–1.
(46) Vilan, A.; Shanzer, A.; Cahen, D. *Nature* **2000**, *404*, 166.
(47) Vilan, A.; Ussyshkin, R.; Gartsman, K.; Cahen, D.; Naaman, R.; Shanzer, A. *J. Phys. Chem. B* **1998**, *102*, 3307.
(48) Haick, H.; Ambrico, M.; Ligonzo, T.; Tung, R. T.; Cahen, D. *J. Am. Chem. Soc.* **2006**, *128*, 6854.
(49) Bruening, M.; Moons, E.; Cahen, D.; Shanzer, A. *J. Phys. Chem.* **1995**, *99*, 8368.
(50) Cohen, R.; Kronik, L.; Shanzer, A.; Cahen, D.; Liu, A.; Rosenwaks, Y.; Lorenz, J. K.; Ellis, A. B. *J. Am. Chem. Soc.* **1999**, *121*, 10545.

JP803124J